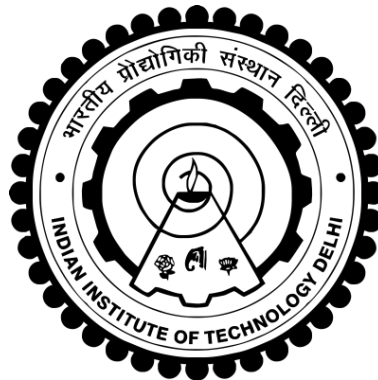


**FLOW CHARACTERISTICS OF AN INLINE-SLOT  
CONICAL EJECTOR-DIFFUSER: AN INFRARED  
SUPPRESSION DEVICE**

**LAKHVINDER SINGH**



**DEPARTMENT OF APPLIED MECHANICS  
INDIAN INSTITUTE OF TECHNOLOGY DELHI  
FEBRUARY 2020**

© Indian Institute of Technology Delhi (IITD), New Delhi, 2020

**FLOW CHARACTERISTICS OF AN INLINE-SLOT  
CONICAL EJECTOR-DIFFUSER: AN INFRARED  
SUPPRESSION DEVICE**

*by*

**LAKHVINDER SINGH**

**Department of Applied Mechanics**

*Submitted*

**in fulfilment of the requirements of the degree of Doctor of Philosophy**

*to the*



**INDIAN INSTITUTE OF TECHNOLOGY DELHI**

**FEBRUARY 2020**

Dedicated to

**My Parents**

**My Wife, Puja**

and

**My Daughter, My Treasure, Kanishka**

# Certificate

This is to certify that the thesis entitled “**Flow Characteristics of an Inline-Slot Conical Ejector Diffuser: An Infrared Suppression Device**”, being submitted by **Lakhvinder Singh** to the Indian Institute of Technology Delhi for the award of the degree of **Doctor of Philosophy**, is a record of the bonafide research carried out by him which has been prepared under our supervisions in conformity with the rules and regulations of the Indian Institute of Technology Delhi. The research reports and results presented in the thesis has not been submitted for any degree or diploma in any other university or institute.

**Dr. S. N. Singh**

Professor

Department of Applied Mechanics

Indian Institute of Technology Delhi

New Delhi - 110016

India

**Dr. Sawan S. Sinha**

Associate Professor

Department of Applied Mechanics

Indian Institute of Technology Delhi

New Delhi - 110016

India

Date:

Place:

# Acknowledgements

With great profoundness and heartfelt reverence, my sincere gratitude to my research supervisors, Prof. S. N. Singh and Dr S. S. Sinha for their valuable time, thoughtful advice and constant support at all level. It is a real privilege and honour for me to share their exceptional knowledge and extraordinary human qualities. My special thanks to Prof. S. N. Singh for sharing his knowledge, experience, fatherly advice, opinions and moral support. His vast knowledge and research expertise have helped me understand, appreciate, evolve and gain deeper insights into my topic. The long and regular discussions helped me get a better idea into the current research, which is the real reasons for the outcome of the present work. Further, throughout my tenure, he has regularly emphasised and helped me become an independent researcher along with a good human being.

My sincere thanks to my co-supervisor Dr S. S. Sinha for his rational and balanced approach, thought-provoking discussions, his readiness to help whenever required. Further, all the discussions I had with him always helped me to remove the ambiguities and brought a sense of clarity in my work. His quality of attention to details has helped me to improve my writing skills immensely. I am profoundly impacted by his teaching style and had the privilege to study course on turbulence and its modelling. The ease with which he explains difficult concepts is exemplary, and I strive to develop similar skills.

I am grateful to the technical staff members of the Gas Dynamics Laboratory, Fluid Mechanics Laboratory and Departmental Workshop. The staff members; Mr Madan Gopal, Mr Suresh Sharma, Mr Manohar Lal, Mr Yogesh Gautam and Mr Kunj Bihari, have rendered their continuous support in setting up my experimental facility without

which the journey would have been arduous. Their contribution will be an everlasting chapter in my memory. A special thank to Mr Manohar Lal for his immense help in setting up the heater arrangement for the hot flow experiments. I also wish to thank Mr Rishav Rajora for his specific input on setting up hot wire anemometer, and Mr Ankur Gupta for assembling components of the diffuser. I wish to thank Dr S. Nasiruddin for his technical inputs and kind cooperation while conducting my experiments. I would also like to thank my work colleague Mr Shrish Shukla and Dr S. Nasiruddin, for their companionship and for providing pleasurable and friendly working atmosphere. My gratitude towards them will always remain for the liberty they gave me to approach them at any point, despite their busy schedule. I cherish all the time spent with them, especially the tea breaks as well as light-hearted conversations throughout my stay at IIT Delhi. I wish to thank my friends Dr Pritanshu Ranjan, Mr Rishav Rajora, Mr Anuj Shukla, Dr Bishweshwar Babu, Mr Rama Kant Singh, Mr Sandeep Yadav, Mr Hamid Hasan, Dr Lokesh Kumar Ragta who stood with me in difficult times. I feel indebted to their love, support and encouragement. I want to thank everyone else who played an essential role in completing this work and also express an apology if I have forgotten to thank someone personally.

I would also like to thank my Institution and my departmental research committee faculty members without whom this research work would have been a remote reality.

No words can express my deep sense of gratitude towards my parents for acting as pillars of strength, support and encouragement. Their unflinching love, blessings, encouragement and belief in me and extending support to my wife and daughter, despite all odds and pressures, gave me the strength all the time. I am very grateful to my wife, Puja, for her love, patience and cooperation and taking care of our daughter during the period of research work. It was impossible to complete this degree without her inspiration.

LAKHVINDER SINGH

# Abstract

An infrared suppression system (IRSS) is an indispensable component of combat vehicles such as helicopters, ships, tanks, etc. Ejector diffuser, a passive IRSS device, is employed to suppress the infrared signatures originating from the exhaust gases and heated metal body of these vehicles. The mechanism of IRSS is based on the mixing of hot exhaust gases with the entrained ambient air within the ejector diffuser. Further, it has to recover static pressure such gas turbine performance is not affected. Ejector diffuser is a combination of a standalone ejector and a diffuser with slots. The performance of an ejector diffuser depends upon a larger number of geometrical and dynamical parameters. In spite of knowing the importance of an ejector diffuser for a combat vehicle yet the literature present in the open forum is scanty due to confidential nature of the application. Based on the available literature survey, various shapes of ejector diffuser such as circular, rectangular and oblong has been studied. Also, the effect of some of the geometrical parameters have been reported. However, no work related to the modification of slot shape by providing guidance at the slot has been conducted. The emphasis of the current work is to systematically investigate the various slot configurations such that higher performance can be achieved. The current study is conducted in two phases:

## Experimental Study

Four ejector diffuser configurations are fabricated and are individually tested using a blower test rig. The four ejector diffuser configurations are broadly categorized as (i) inline slot with no guidance at the slot, and (ii) inline slot with guidance at the slot. Within



each category, there are two types of diffusers based on the slot area namely (i) constant slot area and (ii) increasing slot area. Thus the four ejector diffuser configurations are:

1. No guidance at the slot ejector diffuser with constant slot area (NGCA)
2. No guidance at the slot ejector diffuser with increasing slot area (NGIA)
3. Guidance at the slot ejector diffuser with constant slot area (GCA)
4. Guidance at the slot ejector diffuser with increasing slot area (GIA)

The experimental data has been obtained in terms of velocity profiles at multiple locations in the ejector diffuser using Five-hole probe. Static pressure taps are used to obtain wall static pressure. Resistance thermal detectors are used to obtain temperature profile in the case of hot flow conditions. Constant temperature hotwire anemometer is used to calculate nozzle inlet turbulence intensity. The experimental data is analysed to determine the effect of Reynolds number by varying it as  $Re_{nz} = 7.3 \times 10^4$ ,  $Re_{nz} = 1.2 \times 10^5$ ,  $Re_{nz} = 1.8 \times 10^5$ ,  $Re_{nz} = 2.3 \times 10^5$  for GCA. The analysis of flow and mass entrainment characteristics shows that the performance is independent of Reynolds number for the range investigated. Analyses of mass entrainment for all configurations shows that GIA entrains maximum ambient air. Comparison between the increasing slot area and constant slot area shows that the increasing slot area configuration for both the guided-slot and no-guided-slot ejector diffuser entrains higher ambient air. Analysis of static pressure recovery reveals that NGCA and NGIA recover approximately 1.75 times more static pressure compared to GCA and GIA.

## Numerical Study

The numerical methodology adopted to carry out the simulation studies is first validated against the in-house experimental results and with the data available in the literature after having carried out grid sensitivity and order of convergence studies. The numerical results are broadly discussed in terms of local and cumulative mass entrainment ratio,

thermal characteristics, and static pressure recovery. Following numerical investigations are carried out to understand the performance and flow characteristics of the inline slot ejector diffuser:

1. **Optimization of Standalone Ejector:** This study is conducted for a standalone ejector such that the optimized ejector could be used for the complete ejector diffuser. In the first part, effect of nozzle inlet Reynolds number on mass entrainment is carried out for the ejector. The mass entrainment characteristics are found to be independent of Reynolds number when  $Re_{nz} > 10^5$ . In the second part, effect of standoff distance (SD) and mixing tube area ratio ( $AR_{mx}$ ) on the performance of a circular air-air ejector is carried out. Standoff distance is varied in the range of  $1D_{nz} < SD < 4D_{nz}$  where  $D_{nz}$  is the nozzle diameter while the  $AR_{mx}$  is varied over the range  $1.25 < AR_{mx} < 4$ . It is found that the performance of ejector diffuser is independent of SD when  $AR_{mx}$  lies between 2 and 2.5. Analysis of peak velocity at the inlet of mixing tube indicates that the jet does not expand beyond the mixing tube diameter for the ejector configurations having  $1.25D_{nz} \leq SD \leq 2.5D_{nz}$  and  $2.0 \leq AR_{mx} \leq 2.5$ . In the third part, the length of the mixing tube is varied over the range  $4D_{nz} \leq L_{mx} \leq 16D_{nz}$ . It is found that when the mixing tube length exceeds  $8D_{nz}$  it does not affect the performance of ejector. However, longer mixing tube helps in the flow development and the mixing of secondary and primary air.

2. **Investigation of Inline-slot Ejector Diffuser** Systematic studies are carried out to investigate the performance of various configurations of inline-slot ejector diffuser. Following studies are undertaken:

(a) **Effect of Reynolds Number on Ejector Diffuser Performance:** The nozzle inlet Reynolds number is varied in the range of  $4.3 \times 10^4 \leq Re_{nz} \leq 4.2 \times 10^5$ . The local and cumulative mass entrainment ratio variations were within  $\pm 1\%$ , and the variations in  $C_p$  is within  $\pm 1.5\%$ . It is concluded that the performance of inline-slot ejector diffuser is independent of the Reynolds

number when  $Re_{nz} > 4.3 \times 10^4$ .

- (b) **Effect of Guidance at the Slot:** Performance comparison is carried out between the two configurations of inline slot ejector diffusers with guidance at the slot (guided-slot case) and other having no guidance at the slot (no-guided-slot). Keeping all other geometrical and dynamical parameters consistent, the curved-guided-slot case achieves higher cumulative mass entrainment ( $> 3.5\%$ ) as well as lower wall temperatures throughout the diffuser wall (nearly ambient temperature 300K). However, the limitation of the guided-slot case is lower static pressure recovery compared to the no-guided-slot case.
- (c) **Effect of Slot Area:** Another critical design parameter for inline slot ejector diffuser is the slot-area. In this study, the slot-area along the length of the diffuser is varied as a function of the area of the first slot. Three variations are studied as (i) increasing slot area, (ii) constant slot area, and (iii) decreasing slot area. It is found that the performance of increasing slot area configurations is better than constant and decreasing slot area cases.
- (d) **Effect of Slot Guidance Shape:** More variations of the shapes of the guidance at the slot are investigated namely (i) curved guidance at the slot with trailing edge parallel to diffuser wall, (ii) straight plate guidance at the slot. Analysis of the performance shows that significant difference in the performance is observed between the straight plate guidance and curved plate guidance. However, no difference in the performance is observed between the two configuration of curved-plate guidance (Flow exit from the guidance parallel to the diffuser axis or parallel to the diffuser wall).
- (e) **Effect of Straight Plate Inclination:** More configurations of straight plate guidance at the slot are investigated by varying the angle of the plate formed between the slot and diffuser axis over the range  $0^\circ \leq \theta \leq 28^\circ$ . Higher mass entrainment and better thermal characteristics are observed with increasing

plate angle while pressure recovery reduces with increase in plate angle.

- (f) **Study of Hybrid Slot Plate Guidance:** Design modifications to straight plate guidance at the slot is introduced by fusing two plates having angles of  $0^\circ$  and  $28^\circ$ , referred as hybrid slot. Two new design; (i) a hybrid guidance at the first slot only while other slots having straight plate guidance of  $28^\circ$  (Hybrid\_first\_slot) , and (ii) hybrid guidance at all the slots (Hybrid\_all\_slot) are investigated. It is found that the Hybrid\_first\_slot configuration beside higher mass entrainment and better thermal characteristics also recovers maximum static pressure.

## सार

एक इन्फ्रारेड सप्रेसन सिस्टम (IRSS) लड़ाकू वाहनों जैसे हेलीकाप्टरों, जहाजों, टैंकों आदि का एक अनिवार्य घटक है। एक निष्क्रिय IRSS डिवाइस, इजेक्टर डिफ्यूज़र, इन वाहनों के एक्जास्ट गैसों और बाह्य धातु आवरण से उत्पन्न होने वाले इन्फ्रारेड सिग्नल को सप्रेस करने के लिए किया जाता है। IRSS का कार्यतंत्र गर्म एग्जॉस्ट गैसेस और ठंडी वातुनिकुलित हवा के मिश्रण पर आधारित होता है। सामान्यतः गैस टरबाइन इंजन की कार्यप्रणाली इन मिश्रित गैसों के दभाव पर आधारित होती है, जोकि अत्यधिक बाह्य दभाव पर संचारित होती है और इस बाह्य दभाव में परिवर्तन इंजन के कार्यप्रणाली पर प्रतिकूल असर डालती है। इजेक्टर डिफ्यूज़र एक पूर्णत्व इजेक्टर और स्लॉट्स के साथ एक डिफ्यूज़र का संयोजन है। एक इजेक्टर डिफ्यूज़र का प्रदर्शन अनेक ज्यामितीय और गतिशील मापदंडों पर निर्भर करता है। इस प्रणाली की लड़ाकू विमानों में अत्यधिक उपयोगिता के बावजूद बहुत ही कम अवर्गीकृत अनुसन्धान साहित्य मौजूद है। इन उपलब्ध अनुसन्धान साहित्यों के अनुसार, विभिन्न प्रकार के इजेक्टर डिफ्यूज़र मुख्यता वृत्ताकार, आयताकार और अंडाकार आकारों का वर्णन मिलता है। इस के साथ-साथ साथ, कुछ ज्यामितीय मापदंडों के प्रभाव का वर्णन मिलता है। परन्तु डिफ्यूज़र के स्लॉट के आकारों में परिवर्तन के प्रभाव का कोई वृत्तांत नहीं मिलता है। अतः वर्तमान अनुसन्धान कार्य डिफ्यूज़र के विभिन्न स्लॉट आकारों का व्यवस्थित रूप से जांच करने पर केंद्रित है ताकि उच्च कार्यक्षमता प्राप्त की जा सके। वर्तमान अध्ययन की रूपरेखा दो चरणों में प्रयोजित की गयी है।

**प्रायोगिक अध्ययन:** चार इजेक्टर डिफ्यूज़र आकार निर्मित गए हैं और पृथक रूप से विंड टनल का उपयोग करके परीक्षण किए गए हैं। चार इजेक्टर डिफ्यूज़र आकार (i) इनलाइन स्लॉट बिना वक्रता के साथ, और (ii) इनलाइन स्लॉट वक्रता के साथ। प्रत्येक श्रेणी के भीतर, स्लॉट क्षेत्र के आधार पर दो प्रकार के आकार हैं (i) निरंतर स्लॉट आकार और (ii) बढ़ते स्लॉट आकार। इस प्रकार चार इजेक्टर डिफ्यूज़र प्रस्तुत हैं:

1. निरंतर स्लॉट आकार (NGCA) के साथ स्लॉट इजेक्टर डिफ्यूज़र पर कोई वक्रता नहीं
2. बढ़ते स्लॉट आकार (NGIA) के साथ स्लॉट इजेक्टर डिफ्यूज़र पर कोई वक्रता नहीं
3. निरंतर स्लॉट आकार (GCA) के साथ स्लॉट इजेक्टर डिफ्यूज़र पर वक्रता
4. बढ़ते स्लॉट आकार (GIA) के साथ स्लॉट इजेक्टर डिफ्यूज़र पर वक्रता

पंच-छिद्र वायु वेग मापक यन्त्र का उपयोग करके इजेक्टर डिफ्यूज़र में कई स्थानों पर वेग वृतांत के संदर्भ में प्रयोगात्मक आँकड़े प्राप्त किये गए हैं। स्टैटिक प्रेशर टैप का उपयोग करके वॉल स्टैटिक प्रेशर प्राप्त किये गए हैं। प्रतिरोध थर्मल संसूचक गर्म वायु प्रवाह की स्थिति का तापमान वृतांत प्राप्त करने के लिए उपयोग किये गए हैं। सामान-तापमान हॉटवायर-एनीमोमीटर का उपयोग नोजल इनलेट टर्बुलेंस तीव्रता की गणना करने के लिए किया गया है। GCA आकार के लिए प्रायोगिक आँकड़े को रेनॉल्ड्स संख्या  $7.3 \times 10^4$ ,  $1.2 \times 10^5$ ,  $1.8 \times 10^5$ ,  $2.3 \times 10^5$  में लिए गए हैं और रेनॉल्ड्स संख्या में परिवर्तन के प्रभाव की अध्ययन किया गया है। यह अध्ययन का निष्कर्ष हमें अवगत कराता है की रेनॉल्ड्स संख्या में परिवर्तन का कोई गुणात्मक प्रभाव इजेक्टर डिफ्यूज़र की कार्यप्रणाली पर नहीं पड़ता है। सभी आकारों के लिए द्रव्यमान प्रवेश के विश्लेषण से पता चलता है कि GIA आकार अधिकतम वातुनिकुलित वायु का प्रवेश होता है। बढ़ते स्लॉट और निरंतर स्लॉट आकार के बीच तुलना से पता चलता है कि वक्रता स्लॉट आकार और बिना वक्रता स्लॉट आकार इजेक्टर डिफ्यूज़र दोनों के लिए बढ़ते स्लॉट आकारों पर उच्च वातुनिकुलित वायु प्रवेश करते हैं। स्टैटिक प्रेशर रिकवरी के विश्लेषण से पता चलता है कि GCA और GIA की तुलना में NGCA और NGIA में लगभग 1.75 गुना अधिक स्टैटिक प्रेशर मिलता है।

**अभिकलन अध्ययन:** अभिकलन अध्ययन को करने के लिए अपनाई जाने वाली पद्धति को पहले इन-हाउस प्रायोगिक परिणामों के मानदंड के अनुसार मान्य किया गया। साहित्य में उपलब्ध आंकड़ों के साथ ग्रिड-इंडिपेंडेंस और अभिसरण अध्ययन को पूरा किया गया है। अभिकलन परिणामों को स्थानीय और संचयी द्रव्यमान प्रवेश अनुपात, थर्मल विशेषताओं और स्टैटिक प्रेशर रिकवरी के संदर्भ में व्यापक रूप से वृतांत किया गया है। इनलाइन स्लॉट इजेक्टर डिफ्यूज़र के प्रदर्शन और प्रवाह विशेषताओं को समझने के लिए संख्यात्मक जांच के पश्चात:

1. **स्टैंडअलोन इजेक्टर का अनुकूलन:** यह अध्ययन एक स्टैंडअलोन इजेक्टर के लिए किया जाता है, ताकि पूर्ण इजेक्टर डिफ्यूज़र के लिए अनुकूलित इजेक्टर का उपयोग किया जा सके। पहले भाग में, द्रव्यमान प्रवेश पर नोजल इनलेट रेनॉल्ड्स संख्या का प्रभाव इजेक्टर के लिए किया जाता है।  $Re_{nz} > 10^5$  के द्रव्यमान में प्रवेश की विशेषताओं को रेनॉल्ड्स संख्या से स्वतंत्र पाया जाता है। दूसरे भाग में, एक गोलाकार एयर-एयर इजेक्टर के प्रदर्शन पर स्टैंडऑफ़ दूरी (SD) और मिक्सिंग ट्यूब आकार अनुपात ( $AR_{mx}$ ) का प्रभाव होता है। स्टैंडऑफ़ दूरी  $1D_{nz} < SD < 4D_{nz}$  की सीमा में भिन्न होती है, जहां  $D_{nz}$  नोजल व्यास होता है, जबकि  $AR_{mx}$   $1.25 < AR_{mx} < 4$  से विविध होता है। यह पाया जाता है कि इजेक्टर डिफ्यूज़र का प्रदर्शन SD से स्वतंत्र है जब  $AR_{mx}$  के बीच स्थित होता है 2 और 2.5। मिक्सिंग ट्यूब के इनलेट पर उच्च आयाम वेग का विश्लेषण बताता है कि जेट  $1.25D_{nz} \leq SD$

$\leq 2.5D_{nz}$  और  $2.0 \leq AR_{mx} \leq 2.5$  वाले ईजेक्टर आकार के लिए मिक्स ट्यूब व्यास से आगे नहीं बढ़ता है। तीसरे भाग में, मिक्सिंग ट्यूब की लंबाई  $4D_{nz} \leq L_{mx} \leq 16D_{nz}$  की सीमा से अधिक है। यह पाया जाता है कि जब मिक्सिंग ट्यूब की लंबाई  $8D_{nz}$  से अधिक हो जाती है तो यह इजेक्टर करने वाले के प्रदर्शन को प्रभावित नहीं करता है। हालांकि, लंबे समय तक मिक्सिंग ट्यूब प्रवाह के विकास और माध्यमिक और प्राथमिक हवा के मिश्रण में मदद करता है।

2. **इनलाइन-स्लॉट इजेक्टर डिफ्यूज़र की जांच:** इनलाइन-स्लॉट इजेक्टर डिफ्यूज़र के विभिन्न आकारों के प्रदर्शन की जांच के लिए व्यवस्थित अध्ययन किए गए हैं। निम्नलिखित अध्ययन किए गए हैं:

- I. **इजेक्टर डिफ्यूज़र प्रदर्शन पर रेनॉल्ड्स संख्या का प्रभाव:** नोजल इनलेट रेनॉल्ड्स संख्या  $4.3 \times 10^4 \leq Re_{nz} \leq 4.2 \times 10^5$  की सीमा में है। स्थानीय और संचयी द्रव्यमान प्रवेश अनुपात में भिन्नता  $\pm 1\%$  के भीतर और  $C_p$  में भिन्नता  $1.5\%$  के भीतर है। यह निष्कर्ष निकाला गया है कि जब रेनॉल्ड्स  $4.3 \times 10^4$  से अधिक है, तो इनलाइन-स्लॉट इजेक्टर डिफ्यूज़र का प्रदर्शन रेनॉल्ड्स संख्या से स्वतंत्र है।
- II. **स्लॉट पर वक्रता का प्रभाव:** स्लॉट में वक्रता के साथ इनलाइन स्लॉट इजेक्टर डिफ्यूज़र के दो आकारों और स्लॉट में कोई वक्रता नहीं होने के बीच प्रदर्शन की तुलना की जाती है। अन्य सभी ज्यामितीय और गतिशील मापदंडों को समरूप बनाए रखते हुए, घुमावदार-निर्देशित-स्लॉट आकार उच्च संचयी द्रव्यमान प्रवेश ( $> 3.5\%$ ) और साथ ही साथ डिफ्यूज़र आवरण (लगभग परिवेश तापमान 300K) में तापमान को कम करता है। हालांकि, वक्रता-स्लॉट मामले की तुलना में बिना वक्रता-स्लॉट कम स्टैटिक प्रेशर रिकवरी प्राप्त होती है।
- III. **स्लॉट आकार का प्रभाव:** स्लॉट आकार इजेक्टर डिफ्यूज़र के लिए एक महत्वपूर्ण डिजाइन पैरामीटर है। इस अध्ययन में, डिफ्यूज़र की लंबाई के साथ स्लॉट-आकार पहले स्लॉट के आकार के फलन के रूप में विविध है। तीन भिन्नताओं का अध्ययन (i) बढ़ते स्लॉट आकार, (ii) निरंतर स्लॉट आकार, और (iii) स्लॉट आकार में कमी के रूप में किया गया है। यह पाया गया है कि बढ़ते आकार के विन्यास का प्रदर्शन निरंतर और घटते स्लॉट आकार के मामलों से बेहतर है।
- IV. **स्लॉट वक्रता आकार का प्रभाव:** स्लॉट पर वक्रता के आकार की भिन्नता की जांच की गयी है जैसे (i) डिफ्यूज़र दीवार के समानांतर किनारे के साथ स्लॉट में घुमावदार वक्रता, (ii) सीधे स्लॉट में प्लेट वक्रता में की जाती है। इस प्रदर्शन के विश्लेषण से पता चलता है

कि सीधी प्लेट वक्रता और घुमावदार प्लेट वक्रता के बीच प्रदर्शन में महत्वपूर्ण अंतर पाया जाता है। हालांकि, घुमावदार प्लेट वक्रता के दो विन्यासों के बीच प्रदर्शन में कोई अंतर नहीं देखा जाता है (डिफ्यूज़र अक्ष के समानांतर वक्रता से प्रवाह बाहर निकलना या डिफ्यूज़र दीवार के समानांतर)।

- v. **स्ट्रेट प्लेट झुकाव का प्रभाव:** स्लॉट में स्ट्रेट प्लेट वक्रता के अधिक विन्यासों की जांच स्लॉट और डिफ्यूज़र अक्ष के बीच के अंतर को अलग-अलग करके  $0^\circ \leq \theta \leq 28^\circ$  के रेंज में की जाती है। उच्च द्रव्यमान प्रवेश और बेहतर तापीय विशेषताओं को बढ़ते प्लेट कोण के साथ देखा जाता है जबकि स्टैटिक प्रेशर रिकवरी प्लेट कोण में वृद्धि के साथ कम हो जाती है।
- vi. **हाइब्रिड स्लॉट प्लेट वक्रता का अध्ययन:** स्लॉट में स्ट्रेट प्लेट वक्रता के लिए डिजाइन संशोधनों को दो प्लेटों,  $0^\circ$  और  $28^\circ$  के कोणों को जोड़कर पेश किया जाता है, जिसे हाइब्रिड स्लॉट कहा जाता है। दो नए डिजाइन; (i) पहले स्लॉट में एक हाइब्रिड वक्रता केवल जबकि अन्य स्लॉट्स में  $28^\circ$  प्लेट (हाइब्रिड पहला स्लॉट) की सीधी प्लेट वक्रता होती है, और (ii) सभी स्लॉट्स में हाइब्रिड वक्रता (हाइब्रिड सभी स्लॉट) की जांच की गयी है। यह पाया जाता है कि हाइब्रिड पहला स्लॉट आकृति उच्च द्रव्यमान प्रवेश और बेहतर तापीय विशेषताओं के साथ उच्च स्टैटिक प्रेशर रिकवरी भी मिलती है।



# Table of Contents

Certificate	i
Acknowledgements	iii
Abstract	v
Table of Contents	xv
List of Figures	xxi
List of Tables	xxix
Nomenclature	xxxii
<b>1 Introduction</b>	<b>1</b>
1.1 Ejector Diffuser . . . . .	3
1.2 Performance Indicators for an Ejector Diffuser . . . . .	7
1.2.1 Local Mass Entrainment Ratio ( $\kappa$ ) and Cumulative Mass Entrainment Ratio ( $\phi$ ) . . . . .	7
1.2.2 Normalized Temperature Variation ( $\psi$ ) . . . . .	8
1.2.3 Coefficient of Pressure Recovery ( $C_p$ ) . . . . .	8
1.3 Motivation . . . . .	9
1.4 Organisation of the Thesis . . . . .	10

<b>2</b>	<b>Literature Review</b>	<b>13</b>
2.1	Ejector . . . . .	13
2.1.1	Nozzle . . . . .	14
2.1.2	Standoff distance . . . . .	17
2.1.3	Mixing tube . . . . .	18
2.2	Diffuser . . . . .	22
2.2.1	Stalled Diffusers . . . . .	25
2.2.2	Swirl . . . . .	28
2.2.3	Turbulence Intensity . . . . .	30
2.2.4	Inlet Velocity Profile . . . . .	31
2.3	Ejector diffuser . . . . .	33
2.4	Scope of the Present Work . . . . .	38
<b>3</b>	<b>Experimental Methodology</b>	<b>41</b>
3.1	Experimental Setup . . . . .	41
3.2	Design Details of Test Diffusers . . . . .	45
3.2.1	No-guided-slot Diffuser . . . . .	45
3.2.2	Guided-slot Diffuser . . . . .	46
3.2.3	Constant Slot Area . . . . .	48
3.2.4	Increasing Slot Area . . . . .	49
3.3	Instrumentation . . . . .	50
3.3.1	Five Hole Impact Probe . . . . .	50
3.3.2	Wall Static Pressure Taps . . . . .	53
3.3.3	Hot Wire Anemometer . . . . .	54
3.3.4	Resistance Temperature Detectors . . . . .	55
3.4	Air Heater . . . . .	56
3.5	Traverse Mechanism . . . . .	57
3.6	Experimental Procedure . . . . .	58

3.7	Uncertainty Analysis . . . . .	60
<b>4</b>	<b>Experimental Results and Discussion</b>	<b>63</b>
4.1	Nozzle Inlet Conditions . . . . .	64
4.1.1	Axial Velocity Profile . . . . .	64
4.1.2	Turbulence Intensity . . . . .	64
4.2	Effect of Reynolds Number . . . . .	66
4.3	Mass Entrainment Characteristics of the Inline-Slot Ejector Diffusers . .	71
4.4	Flow Characteristics of Inline-Slot Ejector Diffuser . . . . .	74
4.4.1	Flow Characteristics for No-guided-slot Ejector Diffusers . . . . .	74
4.4.2	Comparison of Flow Characteristics for No-guided-slot and Guided- slot Ejector Diffusers . . . . .	77
4.4.3	Comparison of Flow Characteristics for Guided-slot Ejector Diffusers	81
4.5	Static Pressure Recovery . . . . .	83
4.6	Wall Pressure Distribution . . . . .	84
4.7	Mass Entrainment and Flow Characteristics for Hot Flow Conditions . .	87
<b>5</b>	<b>Mathematical Formulation and Validation</b>	<b>91</b>
5.1	Mathematical Formulation . . . . .	92
5.2	Boundary Conditions . . . . .	101
5.3	Wall Treatment . . . . .	102
5.4	Solver Settings . . . . .	104
5.5	Grid Generation . . . . .	105
5.6	Validation of the CFD Methodology . . . . .	107
5.6.1	Validation Study using the Experimental Results of <a href="#">Sen (2008)</a> . .	108
5.6.2	No-Guided Slot Ejector Diffuser . . . . .	110
5.6.3	Guided Slot Ejector Diffuser . . . . .	117
5.6.4	Guided Slot Ejector Diffuser with Hot Flow Conditions . . . . .	121

<b>6</b>	<b>Computational Investigation: Performance of Inline-Slot Ejector Dif-</b>	
	<b>fuser With and Without Curved Guidance</b>	<b>127</b>
6.1	Range of Parameters . . . . .	128
6.2	Optimization of Ejector . . . . .	129
6.2.1	Effect of Reynolds Number on Ejector Performance . . . . .	132
6.2.2	Effect of Mixing Tube Area Ratio and Standoff Distance on Ejector Performance . . . . .	133
6.2.3	Effect of Mixing Tube Length on Ejector Performance . . . . .	138
6.3	Effect of Reynolds Number on the Ejector Diffuser Performance . . . . .	142
6.4	Effect of Guidance at the Slot for an Inline Slot Ejector Diffuser . . . . .	143
6.4.1	Local and Cumulative Mass Entrainment Ratio . . . . .	144
6.4.2	Thermal Characteristics . . . . .	149
6.4.3	Static Pressure Recovery . . . . .	154
6.5	Effect of Slot Area on the Ejector Diffuser Performance With and Without Guidance at the Slot . . . . .	157
6.5.1	Local and Cumulative Mass Entrained Ratio . . . . .	158
6.5.2	Thermal Characteristics . . . . .	163
6.5.3	Static Pressure Recovery . . . . .	168
6.6	Study of Slot Guidance Shapes for an Inline Slot Ejector Diffuser . . . . .	169
6.6.1	Local and Cumulative Mass Entrainment Ratio . . . . .	170
6.6.2	Thermal Characteristics . . . . .	176
6.6.3	Static Pressure Recovery . . . . .	183
<b>7</b>	<b>Computational Investigation: Performance of Inline-Slot Ejector Dif-</b>	
	<b>fuser with Straight Plate Guidance at Slots</b>	<b>185</b>
7.1	Study of Straight Plate Guidance Orientations at the Slot . . . . .	186
7.1.1	Local and Cumulative Mass Entrainment Ratio . . . . .	187
7.1.2	Thermal Characteristics . . . . .	191

7.1.3	Static Pressure Recovery . . . . .	196
7.2	Design Modification of Straight Plate Guidance . . . . .	198
7.2.1	Local and Cumulative Mass Entrainment Ratio . . . . .	199
7.2.2	Thermal Characteristics . . . . .	201
7.2.3	Static Pressure Recovery . . . . .	206
<b>8</b>	<b>Computational Investigation: Effect of Dynamic Parameters on the Performance of Inline Slot Ejector Diffuser</b>	<b>209</b>
8.1	Effect of Turbulence Intensity . . . . .	210
8.1.1	Local and Cumulative Mass Entrainment Ratio . . . . .	210
8.1.2	Thermal Characteristics . . . . .	212
8.1.3	Static Pressure Recovery . . . . .	213
8.2	Effect of Swirl Number . . . . .	214
8.2.1	Local and Cumulative Mass Entrainment Ratio . . . . .	215
8.2.2	Thermal Characteristics . . . . .	216
8.2.3	Static Pressure Recovery . . . . .	218
8.3	Effect of Ambient Temperature . . . . .	219
8.3.1	Local and Cumulative Mass Entrainment Ratio . . . . .	220
8.3.2	Thermal Characteristics . . . . .	222
8.3.3	Static Pressure Recovery . . . . .	224
<b>9</b>	<b>Conclusion and Suggestion for Future Work</b>	<b>225</b>
9.1	Conclusion from Experimental Investigation . . . . .	226
9.1.1	Nozzle Inlet Conditions . . . . .	226
9.1.2	Effect of Reynolds Number . . . . .	227
9.1.3	Mass Entrainment Characteristics for Inline-slot Ejector Diffusers	227
9.1.4	Flow Characteristics for Inline-slot Ejector Diffuser . . . . .	228
9.1.5	Flow and Mass Characteristics for Hot Flow Conditions . . . . .	228
9.1.6	Static Pressure Recovery . . . . .	229

9.2	Computational Investigation . . . . .	229
9.2.1	Optimization of Standalone Ejector . . . . .	229
9.2.2	Effect of Reynolds Number on Ejector Diffuser Performance: . . .	230
9.2.3	Effect of Curved Guidance with Trailing Edge Parallel to the Dif- fuser Axis at the Slot: . . . . .	230
9.2.4	Effect of Slot Area: . . . . .	231
9.2.5	Effect of Slot Guidance Shape: . . . . .	231
9.2.6	Effect of Straight Plate Inclination: . . . . .	232
9.2.7	Study of Hybrid Plate Guidance: . . . . .	232
9.3	Suggestions for Future Work . . . . .	233

**Bibliography** **235**

# List of Figures

1.1	Application of ejector diffuser in a combat vehicles. Source: M/s W. R. Davis Engg. Ltd. (1975) . . . . .	2
1.2	Application of ejector diffuser in a combat vehicles. Source: M/s W. R. Davis Engg. Ltd. (1975) . . . . .	3
1.3	Schematic of an ejector diffuser. . . . .	5
2.1	Schematic of an ejector . . . . .	14
2.2	Half-delta-wing tab at nozzle exit. Source (Carletti <i>et al.</i> , 1995). . . . .	16
2.3	Circular and lobbed nozzles. Source: Hu <i>et al.</i> (2000). . . . .	17
2.4	Vortices formation for circular (left) and lobbed (right) nozzle. Source: Hu <i>et al.</i> (2000). . . . .	17
2.5	Control volume analysis in a mixing tube . . . . .	19
2.6	Internal flow in the mixing tube (Toulmay, 1988b) . . . . .	20
2.7	Common diffuser terminology. . . . .	22
2.8	Common types of diffusers. . . . .	23
2.9	Flow regimes for a straight walled diffuser. Source: Kline (1959) . . . . .	24
2.10	Injection geometry and pressure profile. Duggins <i>et al.</i> (1978) . . . . .	26
2.11	Effect of cylinder rotating speed on $C_p$ (Singhal <i>et al.</i> (2006)) . . . . .	27
2.12	Different configurations of ejector diffuser used in real practice. Source: M/s W. R. Davis Engg. Ltd. (1975). . . . .	33

2.13	Sizeable difference in the geometries of aerospace, land and marine applications. Source: <a href="#">M/s W. R. Davis Engg. Ltd. (1975)</a> . . . . .	34
2.14	Heat signature data of various helicopters. <a href="#">M/s W. R. Davis Engg. Ltd. (1975)</a> . . . . .	35
3.1	Schematic of the experimental setup. . . . .	42
3.2	Actual experimental setup . . . . .	43
3.3	Schematic of no-guided-slot diffuser highlighting the individual cone elements. . . . .	46
3.4	Schematic of the curved guidance at the slot . . . . .	46
3.5	Test geometry of a curved guided-slot ejector diffuser. . . . .	47
3.6	Geometric details of the ejector diffuser . . . . .	49
3.7	Schematic of the five-hole probe. Source: <a href="#">Patel (2014)</a> . . . . .	51
3.8	Calibration curves of five hole probe . . . . .	52
3.9	Schematic of constant temperature hot wire anemometer. Source: <a href="#">Singh (2009)</a> . . . . .	54
3.10	Calibration curve of the constant temperature hot wire anemometer. . . . .	55
3.11	Components of the heater. . . . .	56
3.12	The traverse mechanism with three degree of freedom. . . . .	57
3.13	Data gathering planes. . . . .	58
4.1	Axial velocity profiles at nozzle inlet . . . . .	65
4.2	Normalized axial velocity profiles at eight measurement locations for the guided-slot ejector diffuser. Location description in <a href="#">Figure 3.13</a> . . . . .	68
4.3	Comparison of $\kappa$ as a function of Reynolds number. . . . .	69
4.4	Comparison of $\phi$ as a function of Reynolds number. . . . .	69
4.5	Comparison of local mass entrainment ratio ( $\kappa$ ) for inline-slot ejector diffuser with and without guidance. . . . .	71



4.6	Comparison of cumulative mass entrainment ratio ( $\phi$ ) for inline-slot ejector diffuser with and without guidance. . . . .	72
4.7	Comparison of normalized axial velocity profiles at eight locations for the no-guided-slot ejector diffusers with constant and increasing slot area. Location description in Figure 3.13 . . . . .	76
4.8	Comparison of normalized axial velocity profiles at eight locations for the no-guided-slot and guided-slot ejector diffusers having constant slot area. Location description in Figure 3.13. . . . .	79
4.9	Comparison of normalized axial velocity profiles at eight locations for the increasing and constant slot area guided-slot ejector diffusers. Location description is shown in Figure 3.13 . . . . .	83
4.10	Normalized wall static pressure distribution as function of Reynolds number for the guided-slot ejector diffuser having constant slot area . . . . .	84
4.11	Wall static pressure for all configurations of inline-slot ejector diffuser. . . . .	85
4.12	Comparison of $\kappa$ for the hot and cold flow conditions for the constant slot area configuration of the guided-slot ejector diffusers. . . . .	87
4.13	Comparison of $\phi$ for the hot and cold flow conditions for the constant slot area configuration of the guided-slot ejector diffusers. . . . .	87
4.14	Comparison of normalized axial velocity profiles at eight locations for the hot and cold flow conditions for guided-slot ejector diffuser having constant slot area configuration. Location description in Figure 3.13 . . . . .	89
5.1	2D axi-symmetric computational domain and boundary conditions for an ejector diffuser. . . . .	101
5.2	Near wall region (Source: <a href="#">ANSYS Academic Research Fluent (Release 15.0)</a> ).103	
5.3	Quadrilateral mesh elements. . . . .	105
5.4	Plot of $y+$ at the wall of ejector diffuser. . . . .	105
5.5	Axial velocity profile comparison downstream of 3 <sup>rd</sup> slot. . . . .	106

5.6	Grid convergence for the three grids and order of convergence as second order scheme. . . . .	107
5.7	2D axi-symmetric computational domain of the ejector diffuser. . . . .	109
5.8	Meshed 2D axi-symmetric computational domain. . . . .	109
5.9	Comparison of axial velocity profile between the predicted and experimental results of Sen (2008). . . . .	109
5.10	2D axi-symmetric computational domain of the no-guided-slot ejector diffuser. . . . .	111
5.11	Meshing of the no-guided-slot ejector diffuser computational domain. . .	112
5.12	Comparison of numerical and experimental results for the no-guided-slot ejector diffuser at $Re_{nz} = 2 \times 10^5$ . Location description in Figure 3.13 . .	115
5.13	Comparison of cumulative mass entrainment ratio ( $\phi$ ). . . . .	116
5.14	Computational domain and boundary conditions. . . . .	117
5.15	Comparison of numerical and experimental results for the curved-guided-slot ejector diffuser at $Re_{nz} = 2 \times 10^5$ . Location description in Figure 3.13 . . . . .	119
5.16	Comparison of Cumulative mass entrainment between experimental and numerical study. . . . .	120
5.17	Computational domain and boundary conditions. . . . .	122
5.18	Comparison of numerical and experimental results for the curved-guided-slot ejector diffuser under hot flow condition at $Re_{nz} = 2 \times 10^5$ . Location description in Figure 3.13 . . . . .	125
5.19	Comparison of predicted axis temperature with in-house experimental results for constant guided slot area ejector diffuser. . . . .	125
5.20	Comparison of predicted exit temperature across the cross section and in-house experimental results for the guided-slot ejector diffuser having constant slot area. . . . .	126
6.1	Schematic of a straight ejector with its constituent parts. . . . .	130

6.2	2D axi-symmetric computational domain and boundary conditions. . . .	131
6.3	Effect of Re on mass entrainment ratio ( $\phi$ )(Case AR2.25SD2.25 $D_{nz}$ ). . .	132
6.4	Streamlines and velocity contour plots for ejector AR2.25SD2.25 $D_{nz}$ . . .	133
6.5	Flow pattern in the simulation having fixed SD 2.25 $D_{nz}$ and varying $AR_{mx}$ .	134
6.6	Variation of mass entrainment ratio ( $\phi$ ) with changing $AR_{mx}$ at fixed SD = 2.25 $D_{nz}$ . . . . .	135
6.7	Variation of mass entrainment ratio ( $\phi$ ) with $AR_{mx}$ at different SD. . . .	135
6.8	Variation of mass entrainment ratio ( $\phi$ ) for fixed AR and varying SD. . .	136
6.9	Flow pattern for an ejector having fixed $AR_{mx}=2.25$ and varying SD. . . . .	137
6.10	Velocity profile at different locations in the mixing tube for case AR2.25SD2.25 $D_{nz}$ .	138
6.11	Static pressure distribution along the axis of the ejector case AR2.25SD2.25 $D_{nz}$ . 139	
6.12	Velocity profile comparison at the outlet for varying mixing tube lengths.	140
6.13	Velocity profile comparison at the inlet for varying mixing tube lengths. .	140
6.14	Variation of maximum velocity at inlet of mixing tube. . . . .	141
6.15	Geometric outline for guided-slot and non-guided-slot ejector diffuser. . .	144
6.16	Local mass entrainment ratio for guided-slot and no-guided-slot ejector diffusers. . . . .	145
6.17	Cumulative mass entrainment ratio for guided-slot and no-guided-slot ejec- tor diffuser. . . . .	145
6.18	Axial velocity at the core of ejector diffuser. . . . .	146
6.19	Static pressure contours near the standoff zone. . . . .	146
6.20	Static pressure contours inside diffuser part. . . . .	147
6.21	Axial velocity downstream of 1 <sup>st</sup> slot. . . . .	147
6.22	$\psi$ along the axis of ejector diffuser. . . . .	150
6.23	Temperature contour inside the diffuser part. . . . .	150
6.24	Showing line sections where results have been extracted. . . . .	151

6.25 Comparison of $\psi$ at multiple locations inside diffuser. Location description is shown in Figure 6.24. . . . .	152
6.26 Ejector diffuser wall temperature distribution. . . . .	153
6.27 Streamlines for guided-slot and no-guided-slot ejector diffuser. . . . .	154
6.28 $C_p$ at different axial location along the ejector diffuser for NGCAED and GCAED. . . . .	155
6.29 Static pressure distribution around 1 <sup>st</sup> slot region for GCAED and NGCAED. . . . .	156
6.30 Comparison of $\kappa$ for Set-I. . . . .	159
6.31 Comparison of $\kappa$ for Set-II. . . . .	159
6.32 Pressure contour for GIAED, GCAED and GDAED. . . . .	160
6.33 Pressure contour for NGIAED, NGCAED and NGDAED. . . . .	160
6.34 Comparison of $\phi$ for Set-I. . . . .	161
6.35 Comparison of $\phi$ for Set-II. . . . .	161
6.36 $\psi$ at ejector diffuser axis for Set-I. . . . .	162
6.37 $\psi$ at ejector diffuser axis for Set-II. . . . .	162
6.38 Comparison of $\psi$ at multiple locations inside diffuser . . . . .	164
6.39 Comparison of $\psi$ at multiple locations inside diffuser . . . . .	165
6.40 Normalized wall temperature. . . . .	166
6.41 Comparison of $C_p$ . . . . .	168
6.42 Schematic diagram of the guidance at the first slot of the ejector diffuser (Table 6.5). . . . .	170
6.43 $\kappa$ for all cases. . . . .	171
6.44 $\phi$ for all cases. . . . .	171
6.45 Static pressure contours at SD. . . . .	172
6.46 Static pressure contours within diffuser. . . . .	173
6.47 Axial velocity downstream of first slot. . . . .	174
6.48 Core temperature variation comparison for the four ejector diffuser. . . . .	176
6.49 Comparison of $\psi$ at multiple locations inside diffuser. . . . .	178

6.50	Temperature contours for slot shapes. . . . .	180
6.51	Streamlines downstream of first slot. . . . .	181
6.52	Wall temperature for the four cases. . . . .	182
6.53	Static pressure recovery. . . . .	183
7.1	Five straight-plate-guide ejector diffusers configurations. . . . .	186
7.2	$\kappa$ for all cases. . . . .	187
7.3	$\phi$ for all cases. . . . .	188
7.4	Pressure contour near standoff distance for all cases. . . . .	189
7.5	Pressure contours inside diffuser section for all cases. . . . .	190
7.6	Axial velocity downstream of third slot. . . . .	191
7.7	Centreline axis temperature comparison for varying straight plate orientations. . . . .	192
7.8	Temperature contour comparison for varying straight plate orientations. . . . .	193
7.9	Comparison of $\psi$ at multiple locations inside diffuser. . . . .	194
7.10	Ejector diffuser non-dimensional wall temperature for all cases. . . . .	196
7.11	Static pressure recovery for ejector diffuser with different plate angle. . . . .	197
7.12	Schematic of a hybrid slot. A combination of $28^\circ$ and $0^\circ$ straight plate guide angles. . . . .	199
7.13	Cumulative mass entrainment ratio . . . . .	200
7.14	Cumulative mass entrainment ratio . . . . .	200
7.15	Centreline axis temperature comparison for varying straight plate orientations. . . . .	202
7.16	Comparison of $\psi$ at multiple locations inside diffuser . . . . .	203
7.17	Comparison of streamlines in hybrid slots cases to straight plate guided slot case. . . . .	204
7.18	Ejector diffuser non-dimensional wall temperature for all cases. . . . .	205
7.19	Comparison of $C_p$ for the hybrid slot ejector diffuser. . . . .	206

8.1	Cumulative mass entrainment ratio as function of inlet turbulence intensity	211
8.2	Comparison of $\psi$ profiles at ejector diffuser exit as function of turbulence intensity. . . . .	212
8.3	Comparison of ejector diffuser wall temperatures in terms of $\psi$ profiles as a function of turbulence intensity. . . . .	213
8.4	Static pressure recovery coefficient for varying nozzle inlet turbulence intensity. . . . .	214
8.5	Cumulative mass entrainment ratio as function of swirl number . . . . .	216
8.6	Comparison of core temperature as function of swirl number. . . . .	217
8.7	Comparison of ejector diffuser exit temperature as function of swirl number.	217
8.8	Comparison of ejector diffuser wall temperature as function of swirl number.	218
8.9	Static pressure recovery coefficient for varying nozzle inlet swirl number.	219
8.10	Comparison of $\kappa$ for all the cases. . . . .	220
8.11	Comparison of $\phi$ for all the cases. . . . .	221
8.12	Comparison of density field in Case A and Case F. . . . .	221
8.13	Normalized temperature variation at ejector diffuser exit. . . . .	223
8.14	Comparison of static pressure recovery for all the cases. . . . .	223

# List of Tables

4.1	Details of Reynolds number, axial velocities, and Mach number . . . . .	66
4.2	Cases description of the inline-slot ejector diffuser . . . . .	71
4.3	Coefficient of static pressure recovery $C_p$ for all configuration of inline-slot ejector diffuser . . . . .	83
5.1	Description of the labels used in the computational domain of an no-guided-slot ejector diffuser . . . . .	112
6.1	Value of the geometric parameters for the optimized ejector diffuser. $D_{nz}$ is the nozzle exit diameter. . . . .	128
6.2	Description of the location in the mixing tube. . . . .	138
6.3	Variation of the performance parameters at various Reynolds number for a curved-guided-slot ejector diffuser . . . . .	142
6.4	Slot area values. IA(Increasing slot area), CA (Constant slot area), DA(Decreasing slot area). . . . .	157
6.5	Configurations of the ejector diffusers . . . . .	169
6.6	$\kappa$ at each opening for the four cases . . . . .	175
7.1	Five configurations of ejector diffusers with straight plate guidance at the slot. . . . .	187
7.2	Ejector diffuser configuration having hybrid slots. . . . .	199
8.1	Case description for studying the varying inlet turbulence intensity . . . . .	210

8.2	Comparison of local mass entrainment ratio ( $\kappa$ ) as a function of turbulence intensity . . . . .	211
8.3	Cases investigated as a function of swirl number . . . . .	215
8.4	Comparison of local mass entrainment ratio ( $\kappa$ ) . . . . .	215
8.5	Cases for the current investigation . . . . .	220



# Nomenclature

## Notations

$C_p$	coefficient of pressure recovery
$c_p$	specific heat at constant pressure
$c_v$	specific heat at constant volume
$D_H$	hydraulic diameter
$e$	internal energy
$e_0$	total energy
$k$	turbulent kinetic energy
$m_{in}$	nozzle exit mass flow rate
$m_{je}$	entrained mass flow rate through slot openings
$p$	static pressure
$p_{ex}$	mass weighted averaged static pressure at the exit
$p_{in}$	mass weighted averaged static pressure at the inlet
$q$	inlet dynamic pressure
$R$	gas constant
$r$	grid refinement factor
$Re$	Reynolds number
$S_{ij}$	mean strain rate tensor
$u', v', w'$	velocity fluctuation in the x, y, z directions
$u_\tau$	wall shear stress
$y^+$	dimensionless distance of the first cell height from the wall

D	diameter of a component
L	length of a component
m	mass flow rate at a cross section
N	total grid size
S	swirl number
T	temperature of the fluid
U	mean flow velocity

### **Greek Symbols**

$\alpha$	Velocity profile shape parameter
$\delta_{ij}$	Kronecker delta
$\epsilon$	turbulent dissipation energy
$\gamma$	inclined manometer angle
$\kappa$	local mass entrainment ratio
$\lambda$	thermal conductivity
$\lambda_t$	turbulent thermal conductivity
$\mu$	dynamic viscosity of the fluid
$\mu_t$	turbulent dynamic viscosity
$\omega$	specific dissipation rate
$\phi$	cumulative mass entrainment ratio
$\psi$	normalized temperature variation
$\rho$	density of the fluid
$\theta$	angle between straight plate guidance and diffuser axis

### **Subscripts**

<i>in</i>	nozzle inlet section
<i>je</i>	slot number
<i>nz</i>	nozzle inlet plane
<i>pl</i>	plenum
0	ambient conditions

$g$  exhaust gas temperature at the nozzle inlet  
mx mixing tube  
tp tailpipe

### **Abbreviation**

AR area ratio  
GCA guidance at the slot ejector diffuser with constant slot area  
GI grid index  
GIA guidance at the slot ejector diffuser with increasing slot area  
IRSS infrared suppression system  
NGCA no guidance at the slot ejector diffuser with constant slot area  
NGIA no guidance at the slot ejector diffuser with increasing slot area  
SD standoff distance  
SIMPLE semi implicit method for pressure linked equations  
TI turbulence intensity